ELSEVIER

Biophysical Chemistry 125 (2007) 375–387

Biophysical Chemistry

http://www.elsevier.com/locate/biophyschem

A theoretical elucidation of bilirubin interaction with HSA's lysines: First electrostatic binding site in IIA subdomain

Zainab Moosavi-Movahedi [a,b], Homayoon Bahrami [a,b], Mansour Zahedi [a,*], Karim Mahnam [b], Jamshid Chamani [b], Shahrokh Safarian [c], Ali A. Saboury [b], Ali A. Moosavi-Movahedi [b]

[a] *Department of Chemistry, Faculty of Sciences, Shahid Beheshti University, Evin, 19839-63113, Tehran, Iran*
[b] *Institute of Biochemistry and Biophysics, University of Tehran, Tehran, Iran*
[c] *Department of Biology, University of Tehran, Tehran, Iran*

Received 29 August 2006; received in revised form 27 September 2006; accepted 27 September 2006
Available online 5 October 2006

Abstract

The electrostatic interaction of amino acid lysines 190, 195 and 199 of human serum albumin (HSA) with bilirubin have been investigated using molecular dynamic simulations, QM and QM/MM minimization methods. In this study two methodological approaches have been employed. In the first approach X-ray structure and the structure obtained from the molecular dynamic simulation of subdomain IIA of HSA in vacuum have been utilized. Interactions have been evaluated with the segment 186–200 of the cited subdomain. Calculations on the X-ray structure of above segment indicate an effective interaction of the lysine 195 with bilirubin, although that of the lysine 190 is also found considerable in this structure. Performing simulation in vacuum, it has been revealed that except for the lysine 195, the other two lysine residues (190 and 199) could not be considered as centers of interaction. Such finding, which is in accord with experimental data, lends support to the procedure employed in this study. NBO analyses suggest that tasks to achieve a structure indicating bilirubin interaction with the lysine 195 from the 186–200 segment extracted from X-ray structure, results in a structure that lacks any electrostatic interaction. In fact, it has been found that the stability of the latter species can be attributed to the H-bonding interaction of the glutamate 188 with both bilirubin and the lysine 195. Further NBO analysis on the structure of the same species, while achieved after molecular dynamic simulation on subdomain IIA in vacuum has revealed that a favorable electrostatic interaction between the lysine 195 and bilirubin has occurred. Besides, H-bonding interaction of the glutamate 188 with bilirubin has been evident in the same species. For the second approach, presence of water molecules and ions has been considered to simulate condensed medium. Applying docking, conformational sampling, and QM/MM minimization steps in sequence, a structure has been achieved which presents a specific interaction between ε-$NH3^+$ group of the lysine 195 residue and the lactam oxygen atom of bilirubin. NBO analyses suggest that above electrostatic interaction is combined with hydrogen bonding interaction between same two groups. Moreover, a hydrogen bond between oxygen atom of bilirubin's acetate group and α-NH group of lysine 195 has been observed. Molecular orbital calculations have been presented which support the NBO analyses.

Keywords: HSA; Bilirubin; Lysine 195; Molecular dynamic simulation; QM/MM minimization; NBO

1. Introduction

Binding analysis of bilirubin (as a toxic metabolite of heme) to the human serum albumin (HSA), as an important carrier of bilirubin in plasma, has been studied for many years [1–6]. Jacobsen has postulated the presence of two types of bilirubin binding sites on HSA. The first type includes a high affinity binding site and the second has two low affinity binding sites [7]. The number of binding sites and their binding affinities changes with salt concentration [8].

Analysis of the amino acid residues involved in bilirubin binding has been studied by modifying certain amino acid residues of HSA via chemical modification. It has been reported that modification of histidine, arginine and tyrosine residues reduces the bilirubin binding affinity on HSA [9]. Another study has proposed the electrostatic attraction between the positive charged amino acid residues, mostly lysine or arginine, and the

* Corresponding author. Tel.: +98 21 22401765; fax: +98 21 22403041.
E-mail address: m-zahedi@cc.sbu.ac.ir (M. Zahedi).

0301-4622/$ - see front matter © 2006 Elsevier B.V. All rights reserved.
doi:10.1016/j.bpc.2006.09.013

negative charges induced on the lactam oxygen atoms of bilirubin [10]. Evidence has been presented for the existence of at least one lysine residue in or close to the high affinity binding site for bilirubin [11]. One investigation has claimed to verify the importance of lysine in the binding process by acetylating all the lysine residues in HSA and showing a dramatic reduction in bilirubin affinity [12]. Although a further such study has shown a reduction in bilirubin affinity only when lysine residues are buried [13]. It has been revealed that the high affinity binding site is located at or near loop 4 in subdomain IIA of the HSA structure [14]. IIA subdomain, which corresponds approximately to amino acid position of 190–300, is one of the two principal sites on HSA for small hydrophobic ligands [15,16]. The proteolytic studies have clarified that the region corresponding to amino acid positions of 186–238 retained the ability to bind bilirubin [17]. However, another study has indicated that the region corresponding to amino acid positions of 240–258 is critical for bilirubin binding to HSA [18]. It has been also proposed that flexible binding sites for bilirubin on HSA can be possible [19]. Binding of bilirubin has been established by various non-covalent forces such as salt linkages, hydrogen bonds, aromatic π−π and hydrophobic interactions [9,20]. It has been determined that salt linkages between carboxyl groups of bilirubin and ε-NH_2 groups of lysine residues in HSA is more important [18,21,22]. The amino acids lysine 195 and lysine 199 are introduced as positively charged residues while lysine 190 remains neutral as shown in the X-ray crystal structure of HSA [19,23].

This work attempts to determine the primary site of HSA upon interaction with bilirubin using molecular dynamic simulations, QM and QM/MM minimization methods. In order to accomplish such task, two computational schemes have been employed. In the first approach based on previous experimental works, a pre-optimized segment 186–200 of HSA has been chosen and its interaction with bilirubin investigated. The aforementioned segment has once been obtained from X-ray structure of subdomain IIA, while another time has been taken from simulation on subdomain IIA of HSA in vacuum. For the second approach, HSA has been initially placed in a water and ion box. By bilirubin docking primary structures for bilirubin HSA interaction have been obtained. Results achieved from docking treatment have guided us to IIA subdomain dissection of HSA. Advancing with a simulated annealing treatment followed by a QM/MM minimization, a structure for interaction of lysine 195 with bilirubin has been obtained. Our final results indicate that simplification in the first approach does not alter the principal conclusions drawn for the primary HSA interaction site with bilirubin which has been subsequently obtained with more complicated calculations in condensed medium.

2. Computational scheme

Gaussian 98 program revision A-9 [24] was employed for optimization and frequency calculation on the structures. B3LYP/6-31G* and PM3 methods [25–27] were benefited to perform the quantum mechanical calculations. Full optimization without any symmetry restriction was performed using FOPT keyword and the Z-MATRIX with C_1 point group. MASSAGE keyword was also used for achieving the basis set superposition error in evaluating the energy of reactants. HyperChem program version 7 was used to perform the molecular dynamic simulation under the AMBER force field on the IIA subdomain of HSA in vacuum and WebLab viewer was used as graphic environment. Molecular dynamic simulation and MM minimization in condensed medium were performed using GROMACS 3.3.1 [28] package under Gromos force field [29]. QM/MM calculations were carried out by coupling both GROMACS 3.3.1 and MOPAC 7 softwares [30,31]. Vibrational frequency calculations on all species studied confirmed the local minimum geometries on their corresponding potential energy surfaces by having no imaginary frequency. Natural bond orbital (NBO) analysis was employed to obtain the lone pair and anti-bonding hybridization as well as second order interaction energies [32].

3. Results and discussion

Previous studies have indicated that the high affinity binding site of bilirubin interaction with HSA is located at the IIA subdomain [14]. Based on such fact, two approaches have been considered for the present investigation. In the first approach, we have dissected the subdomain IIA from the X-ray structure of HSA, and performed a molecular dynamic simulation in vacuum to achieve local minima structures. Interaction of bilirubin with the lysine residues 190, 195, and 199 of 186–200 segment, selected from the subdomain IIA, have been investigated both before and after the simulation using quantum mechanical calculations. In order to reduce the computational cost, and knowing the fact that ethyl side groups do not intervene in the interaction of bilirubin with lysine residues, they have been replaced by hydrogen atoms. In the second approach, water molecules and ions have been taken into account and docking has been used in order to achieve primary structures suitable for HSA bilirubin interaction. Annealing simulation has been further employed to obtain near local structures for the desired interaction. Finally, QM/MM minimization has been performed in order to achieve a local minimum geometry of the bilirubin–IIA subdomain interaction.

3.1. Study of the interaction of bilirubin with the IIA subdomain dissected from X-ray structure by PM3 method

The amino acid lysine on HSA was selected as an interaction site with bilirubin in accord to the previous studies [11–13]. As a first choice electrostatic interaction of bilirubin with HSA [10], the lysines 195 and 199 being positively charged lysine residues which are located between amino acid positions 186–258 shown in the X-ray crystal structure of HSA [19,23], were considered as the prime electrostatic interaction sites with bilirubin. Realizing the existence of the neutral lysine 190 in the vicinity of the lysines 195 and 199, interaction of the former, while protonated artificially was also studied with bilirubin. In order to reduce the computational cost, the amino acids 186–200 segment, containing lysines 190, 195 and 199 was dissected from the IIA X-ray structure of HSA. This segment as well as bilirubin were individually optimized under the PM3 method.

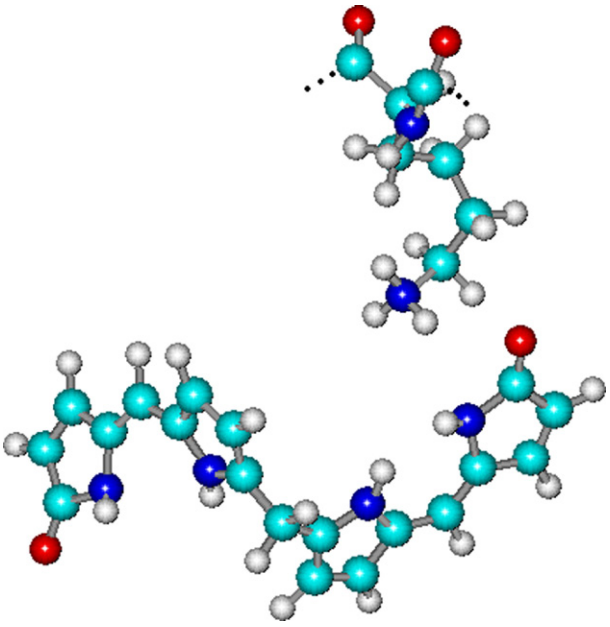

Scheme 1. The optimized structure of bilirubin while interacting with the amino acid lysine 195 in the 186–200 segment (not shown) obtained from X-ray structure of protein. : **C**, : **N**, : **O** and : **H**.

Interaction was allowed to take place while the 186–200 segment was situated nearby bilirubin and optimization was performed with the same method. It should be pointed out that based on chemical intuition, the lactam oxygen atom of bilirubin was located nearby the ε-NH_3^+ of lysine 190, 195 and 199 residues, and computation was carried out once for each amino acid separately. In fact docking of bilirubin to the cited segment was done manually [33]. Scheme 1 shows the optimized structure of bilirubin while interacting with the lysine 195 in 186–200 segment. The energy values of these interactions have been summarized in Table 1. Results indicate that due to destabilization of the amino acid lysine 199 after interacting with bilirubin, this residue could not be considered as a reasonable binding site. As a desirable phenomenon, the influence of a water molecule presenting a specific solvent effect has been considered [33]. Therefore, simultaneous interaction of lysine and bilirubin while accompanied with a water molecule has been investigated. Scheme 2 illustrates the optimized structure of water in the vicinity of bilirubin and the lysine 195 in 186–200 segment. As results in Table 1 reveal, the presence of one water molecule at the vicinity of interaction site may contribute to the system's stability.

Table 1
Interaction energies of bilirubin with the amino acid lysines 190, 195 and 199 of the 186–200 segment obtained from IIA X-ray structure using PM3 method

Interaction	ΔE_{PM3} kJ/mol	
	Without water at interaction center	With water at interaction center
Bilirubin–lysine 190	−267.27	−376.16
Bilirubin–lysine 195	−53.29	−68.22
Bilirubin–lysine 199	101.32	–

3.1.1. Study of interaction of bilirubin with subdomain IIA dissected from X-ray structure by composite calculation method

To have better account of interaction energy of the cited section, it would be wise to employ higher level calculation strategy. However, since 186–200 segment includes more than 230 atoms, performing a full ab initio and DFT quantum mechanical calculation on such a large system seems formidable. Achieving the aforementioned goal, a composite procedure [33,34] which combines both DFT B3LYP/6-31G* and semi-empirical PM3 methods was considered.

In order to carry out this task, the center of interaction, which includes a protonated methyl amine group and bilirubin molecule, must be cut from the previously optimized structure resulted from bilirubin interaction with lysine residues of 186–200 segment by PM3 method. The energies of the mentioned cutout sections were calculated with both PM3 and B3LYP/6-31G* methods. In order to evaluate the energies of interaction in these cut sections, the energies of individual molecules namely protonated methyl amine and bilirubin were calculated after optimization in both PM3 and B3LYP/6-31G* levels. Having all necessary data, the following equation can be employed to calculate the interaction energy for bilirubin with lysine residues of the 186–200 segment:

$$\Delta E_{\text{Composite}}(186\text{–}200 : \text{BIL}) = \Delta E_{\text{PM3}}(186\text{–}200 : \text{BIL}) - \Delta E_{\text{PM3}}(\text{MA} : \text{BIL}) + \Delta E_{\text{B3LYP/6–31G*}}(\text{MA} : \text{BIL}) \quad (1)$$

The composite method, while a water molecule is included in the interaction center leads to the following equation for the interaction energy:

$$\Delta E_{\text{Composite}}(186\text{–}200 : \text{BIL} : \text{H}_2\text{O}) = \Delta E_{\text{PM3}}(186\text{–}200 : \text{BIL} : \text{H}_2\text{O}) - \Delta E_{\text{PM3}}(\text{MA} : \text{BIL} : \text{H}_2\text{O}) + \Delta E_{\text{B3LYP/6–31G*}}(\text{MA} : \text{BIL} : \text{H}_2\text{O}) \quad (2)$$

Where parentheses denote interaction type, and MA and BIL stand for protonated methyl amine and bilirubin respectively.

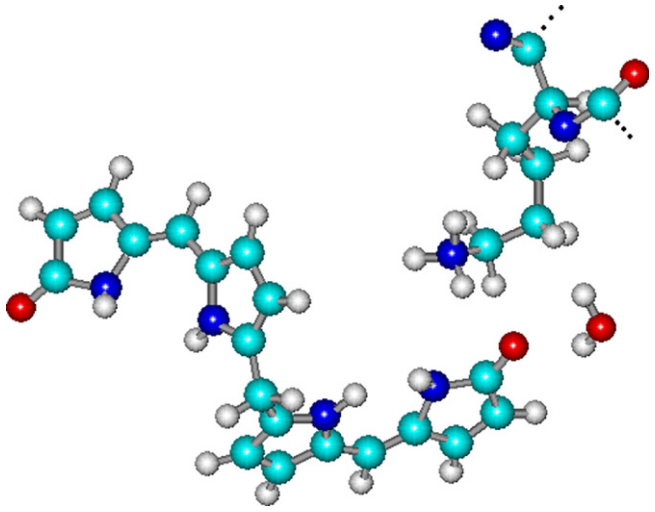

Scheme 2. Optimized structure of bilirubin, one water molecule and the lysine 195 in the 186–200 segment (not shown) obtained from X-ray structure of protein. : **C**, : **N**, : **O** and : **H**.

Results of composite evaluation have been tabulated in Table 2. Basis set superposition error has also been considered in $\Delta E_{\mathrm{B3LYP/6\text{-}31G^*}}$(MA:BIL) of Table 2. Summarized results of Table 2 suggest that the lysine residues 190 and 195 are good candidates as centers of interaction with bilirubin. The same conclusion can be drawn for the interaction energies while a water molecule is also included at the interaction site. Relative binding stability of these residues as well as energy trends acquired by taking advantage of composite method have been discussed in following sections. While working on the optimization of the structures obtained from the interaction of the lysine 195 of 186–200 segment with bilirubin, both with and without the presence of one water molecule at the center of interaction, the intervention of a carboxylate group from glutamate residue 188 was noticed. In order to evaluate the influence of this group, composite calculations just for the lysine 195 was repeated. The interaction energies for such study have been calculated using Eqs. (3a) and (3b) and results summarized in Table 2.

$$\begin{aligned}\Delta E_{\mathrm{Composite}}(186\text{–}200 : \mathrm{BIL} : \mathrm{AC}) &= \Delta E_{\mathrm{PM3}}(186\text{–}200 : \mathrm{BIL} : \mathrm{AC}) \\ &\quad -\Delta E_{\mathrm{PM3}}(\mathrm{MA} : \mathrm{BIL} : \mathrm{AC}) \\ &\quad + \Delta E_{\mathrm{B3LYP/6-31G^*}}(\mathrm{MA} : \mathrm{BIL} : \mathrm{AC})\end{aligned} \tag{3a}$$

$$\begin{aligned}\Delta E_{\mathrm{Composite}}(186\text{–}200 : \mathrm{BIL} : \mathrm{AC} : \mathrm{H_2O}) &= \Delta E_{\mathrm{PM3}}(186\text{–}200 : \mathrm{BIL} : \mathrm{AC} : \mathrm{H_2O}) \\ &\quad -\Delta E_{\mathrm{PM3}}(\mathrm{MA} : \mathrm{BIL} : \mathrm{AC} : \mathrm{H_2O}) \\ &\quad + \Delta E_{\mathrm{B3LYP/6-31G^*}}(\mathrm{MA} : \mathrm{BIL} : \mathrm{AC} : \mathrm{H_2O})\end{aligned} \tag{3b}$$

Where AC denotes acetate group.

By taking a closer look at Table 2, it becomes clear that by considering the interference effect of acetate group in estimating the interaction energy, binding of bilirubin to the lysine 195 has been weakened with no noticeable influence imparted due to water molecule present.

3.2. Simulating subdomain IIA by molecular dynamic in vacuum

From previous discussions it has been revealed that the lysine residues 190 and 195 can be considered as species involved in the interaction center with bilirubin. However, lysine 199 binding interaction to bilirubin does not seem fruitful. As has been presented in above discussions, the most favored binding interaction is presumably found for artificially protonated lysine 190 with bilirubin. On the other hand, comparison of the interaction energies of the lysines 190 and 195 (Tables 1 and 2) to that of experimental reported value of ~60 kJ/mol [11,35] suggest that better correspondence exists for the lysine 195 to experiment. At the same time, when the glutamate 188 interference in the lysine 195–bilirubin interaction has been considered aiming to advance the computational approach, it has been observed that the aforementioned interaction becomes diminished (Table 2). Putting all these points together, we led to the conclusion that in order to come closer to the experimental result for lysine–bilirubin interaction energy, an alternative local minimum geometry for the 186–200 segment would be desired. Therefore, a molecular dynamic simulation of subdomain IIA was performed. Although such simulation in solvent environment can approach our desired structure via many local minima, but only a small segment of phase space (without solvation and polarization effects of solvent) will be scanned in vacuum to achieve fewer minima. Due to distinct energy difference of three lysines residues interacting with bilirubin, we have been initially directed to a simulation of IIA subdomain in vacuum which greatly reduces the calculation cost. Parameters of molecular dynamic simulation performed under the AMBER force field were: 300 K temperature, 350 ps heating time, 0.5 fs time step, 450 ps equilibrium time, and simulation duration of 800 ps. The switch potential was used as a cutoff nonbonding interaction. The plot of RMS values of bond distances versus the simulation time has been shown in Fig. 1. As it is seen from Fig. 1, the RMS values at simulation duration is much less than 1 Å, which is an indication that the simulation is correct and there is no critical situation at bond distances in simulation [36].

Considering the energy changes versus time in the simulation duration and by employing snapshots, the most stable structures of subdomain IIA were extracted. From each selected snapshot, the 186–200 segment was dissected and optimized using PM3 method. The most stable segment turned out to be the one at 750 ps of the simulation period (called '750 ps snapshot' elsewhere).

Table 2
Interaction energies of bilirubin with the amino acid lysines 190, 195 and 199 of the 186–200 segment obtained from IIA X-ray structure using composite method

Interaction	$\Delta E_{\mathrm{Composite}}$ kJ/mol			
	Without acetate group of glutamate 188		With acetate group of glutamate 188	
	Without water at interaction center	With water at interaction center	Without water at interaction center	With water at interaction center
Bilirubin–lysine 190	−232.07	−332.77	–	–
Bilirubin–lysine 195	−90.83	−101.70	−29.09	−27.71
Bilirubin–lysine 199	139.82	–	–	–

3.2.1. Study of bilirubin interaction with the '750 ps snapshot' by PM3 method

Interactions of bilirubin and the lysine residues 190, 195, and 199 in the 186–200 segment with and without one water molecule present were studied similar to Section 3.1. Focusing on the lysine 190, optimization of a non-protonated form of ε-NH_2 of this amino acid in the above segment was fruitless. What observed instead was a transfer of the added proton to the carboxylate group in ε-NH_2 vicinity. Thus in accord with experimental reports, an electrostatic interaction could not occur between the lysine 190 and bilirubin and this amino acid was ignored from any further consideration. It turns out that based on obtained results; simulation in vacuum has been successful in evaluating the relative interaction of the three lysine residues with bilirubin.

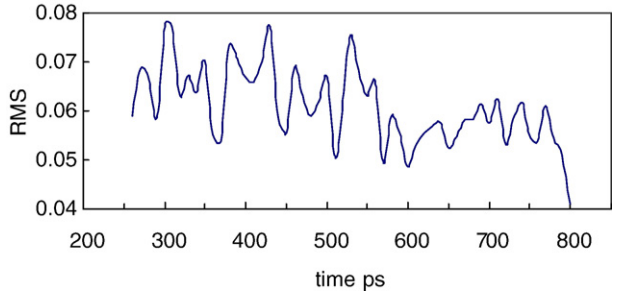

Fig. 1. The plot of RMS values of bonding distance versus the simulation time.

Considering the lysine 199 by looking closer at the '750 ps snapshot', it became evident that due to folding occurred after simulation, the lysine 199 was hidden to the extent that its interaction area with bilirubin was reduced to a great amount. Thus further tasks to obtain an optimized structure showing any effective interaction of this amino acid and bilirubin was fruitless. As a sign of strength of these computational findings, we undoubtedly claim that any electrostatic interaction of the lysine 199 with bilirubin is out of the question.

From above observations, what has been left as a possible binding site of interaction to bilirubin is the lysine 195 alone. Results of the latter lysine and bilirubin interaction have been compiled in Table 3. Same trend as those of Table 1 have been observed in this case except that the energy stability has been raised by about 53 and 45 kJ/mol for cases with and without a water molecule present, respectively.

3.2.2. Investigation of bilirubin interaction with the '750 ps snapshot' by composite method

According to the description presented in Section 3.1.1 and based on Eqs. (1), (2), (3a), and (3b), DFT method was included as an improvement in the computations in order to investigate bilirubin interaction with the lysine 195. Energies of above interaction have been summarized in Table 4. Trends on interaction energies with and without a water molecule present at the binding center are similar to those summarized in Table 2. However, as it is revealed from results of Table 4 while compared to those of Table 2, the electrostatic interactions are stabilized by about 63 kJ/mol. By considering the intervening influence of the glutamate 188 in the above interaction using composite method (Table 4), it is evident that contrary to the results of Section 3.1.1 (Table 2), a favorable binding interaction with an energy stabilization of about 40 kJ/mol has been obtained. Again, as has been mentioned earlier, presence of a water molecule has no noticeable influence in the electrostatic interaction while the profound effect of the glutamate 188 is evident.

Table 3
Interaction energies of bilirubin with the amino acid lysine 195 of the186–200 segment obtained from the IIA Molecular Dynamic (MD) simulated structure using PM3 method

Interaction	$\Delta E_{\text{PM3 MD}}$ kJ/mol
Bilirubin–lysine 195	−98.19
Bilirubin–lysine 195–H_2O	−121.30

Table 4
Interaction energies of bilirubin with the amino acid lysine 195 of the 186–200 segment obtained from the IIA Molecular Dynamic (MD) simulated structure using composite method

Interaction	$\Delta E_{\text{composite MD}}$ kJ/mol	
	Without acetate group of glutamate 188	With acetate group of glutamate 188
Bilirubin–lysine 195	−154.12	−208.46
Bilirubin–lysine 195–H_2O	−165.07	−206.45

3.3. Study of the interaction of bilirubin with subdomain IIA in solution

As has been pointed out earlier, based on the simulation in vacuum results, it is expected that accounting the condensed medium would not affect the relative interaction behavior of lysine residues with bilirubin, namely it is just sufficient to consider the lysine 195 interaction. But more accurate evaluation of the above interaction in condensed medium is required. This is because a more extensive portion of potential energy surface of the above interaction can be scanned, leading to a higher flexibility of determining the interaction sites desired.

3.3.1. Docking

Docking has been performed in arriving at initial structure(s) for the bilirubin–HSA interaction. To have a HSA species which mimics natural characters, a detailed equilibration procedure was carried out as explained below. The X-ray structure of HSA was placed in a solvent box with 29,444 spc216 water molecules being equal to a 9 Å distance for HSA to the box edges. It should be emphasized that among three lysine residues 190, 195 and 199, only the lysine 195 is protonated based on experimental studies. Neutralization of the system required addition of 24 Na^+ ions. In order for water molecules to adapt themselves to the potential due to presence of HSA molecule, by fixing the latter's structure, a structural minimization calculation was performed followed by molecular dynamics simulation for 20 ps with a step time of 1 fs. By relaxing the protein and taking advantage of steepest descent of 1000 steps followed by conjugate gradients of 9000 steps methods, the whole system was minimized. In order to obtain an equilibrium geometry at 300 K and 1 atm, the system was heated by a weak coupling with parameters of 0.1 and 0.5 for temperature and pressure respectively, while heating time for molecular dynamic simulation at 100 K, 200 K and 300 K chosen to be 20 ps. The above simulations were all performed at constant temperature and pressure with a non-bonded cutoff of 16 Å. By achieving the latter equilibrium HSA structure in solvent, bilirubin docking was carried out using a standard autodock software. Docking results suggest that bilirubin–HSA interaction predominantly occurs in IIA subdomain. The sites of these interactions are observed to be formed of two main groups. One in an area between lysines 195 and 199 and glutamates 13 and 15, while the second far from the first and somewhere around lysine 190. Our basis for selecting a structure of each docked group just mentioned has been the score determined based on the energy function and occurrence probability calculated by the docking software. It is apparent that the docking treatments performed here

have the advantage of providing more flexibility and diversity for the bilirubin–HSA interaction compared with the manual docking.

3.3.2. Conformational sampling

As it is apparent, the structures obtained from docking process are a primitive view of the desired HSA–bilirubin interaction. In order to obtain local minimized geometries for such interaction, conformational sampling on selected docked geometries is necessary. To carry out such task, a known technique called simulated annealing method was employed. Both starting structures were obtained based on two main interaction locations mentioned in docking. As has been justified by others and in order to decrease the calculation cost, IIA subdomain of HSA along with bilirubin were bisected from the mentioned structures. Each of the two starting structures was placed in a solvent box with 6839 spc216 water molecules again maintaining a distance of 9 Å to the box edges. Neutralization of the system required addition of 17 Na^+ ions. As was mentioned in docking section, a solution and heating treatment up to 500 K was performed on both systems keeping all simulation parameters the same as before. Annealing treatment on these two equilibrated systems was performed. The strategy being decrease in temperature from 500 K to 50 K followed by increase from 50 K back to 500 K. Time duration for each increase or decrease of temperatures was 50 ps. This way carrying out a simulated annealing of 1 ns resulted in 10 near local minima structures for each starting system. Inspection of the annealed systems showed no indication of any bond breakage or tension in structures as expected. Besides, looking closely at some of the near local minima structures revealed that bilirubin maintained a good interaction with IIA, suggesting that using a temperature as high as 500 K did not have any effect in destroying such interaction.

3.3.3. QM/MM minimization

In order to obtain local minima structures the annealed near local geometries were optimized by taking advantage of steepest descent of 1000 steps followed by conjugate gradients of 9000 steps methods. To achieve a better description of IIA subdomain–bilirubin interaction, minimization of the latter optimized geometries were performed by employing a combination of Gromos force field and PM3 semiempirical methods. Bilirubin as well as residues such as lysines 195, 199, and 190 were treated as QM portion for the minimization. Among twenty final optimized structures, several were irrelevant due to either showing no interaction or presenting bond breakage in bilirubin. One of them appeared to introduce the most desired interaction. The reasoning behind choosing this latter geometry was the fact that it showed interactions with bilirubin from both α-NH and ε-NH_3^+ sites of lysine 195, rather than indicating just one site for interaction as in the remaining geometries. The interaction core extracted from above geometry has been illustrated in Scheme 3. As is evident from this scheme, lysine 195, 199, and glutamate 13 along with bilirubin have been shown. It is clearly apparent that most vicinity is observed for lysine 195 with bilirubin. The interaction due to this neighboring can be assigned to two sites. One site suggests an interaction between H atom of ε-NH_3^+ group of lysine 195 to lactam oxygen of bilirubin, while the other site refers to interaction of oxygen atom of –COO group of bilirubin to H of α-NH group in lysine 195. As has been the case in the first interaction approach, no water molecule is seen to intervene in the interaction medium while lysine 199 has no role in interacting with bilirubin either. It is worth recalling that the prohibitive effect of glutamate 188 on the interaction of lysine 195 with bilirubin had been reduced while simulation in vacuum was performed. Now with simulation carried out in condensed medium, not only such effect has been totally removed but results suggest that although bilirubin could essentially show interaction with all lysine residues as well as glutamates 13, the only apparent remaining bilirubin interaction is with lysine 195. Comparison of Scheme 3 with Schemes 1 and 2 (gas phase structures) reveal the important fact that the atomic configuration in the interaction core is distinguishingly different. Although the gas phase results obtained in this work are acceptable, but if there were not such a large difference between lysine residues behavior in interacting with bilirubin, the mentioned results could be wrong even in a qualitative sense. In order to come up with reasonable explanations for some of the results which have been presented so far, natural bond orbital analysis has been offered in the following section.

3.4. Natural bond orbital (NBO) analysis

In order to discuss about interactions of bilirubin with the lysines 199 and 195 of HSA, it would be informative to investigate the interaction between atomic orbitals, bond orbitals and lone pair orbitals by using NBO analysis. Such analysis gives information regarding interactions like hydrogen bonding, strong van der Waals and hyper-conjugation effects. It is noteworthy that NBO results have been obtained for the dissected segments employed in composite calculation method (Sections 3.1.1 and 3.2.2) as well as for the interaction core introduced in the previous

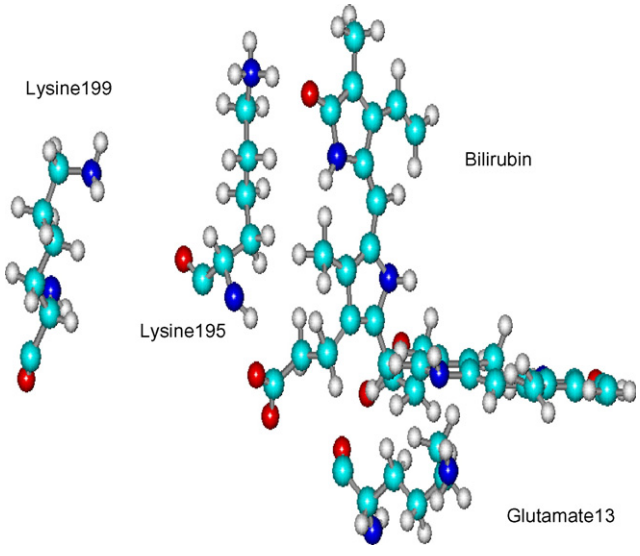

Scheme 3. Optimized core interaction structure obtained from condensed medium calculations: **C**, **N**, **O** and **H**.

Table 5
Hybridization of some lone pair for interaction of bilirubin with the amino acid lysines 195 and 199 of the 186–200 segment

Lone pair	Lys199-bil[a]	Lys195-bil[a]	Lys195-bil-MD[b]	Lys195-bil-MD[c]
Lp(1) O1	$sp^{1.02}$	–	–	$sp^{0.72}$
Lp(2) O1	$sp^{11.57}$	–	–	–
Lp(1) O2	–	–	$sp^{0.94}$	–
Lp(2) O2	–	$sp^{15.68}$	$sp^{10.36}$	–
Lp(1) O3	–	$sp^{0.82}$	–	–
Lp(2) O3	–	$sp^{9.29}$	–	–
Lp(2) O4	–	–	–	p

[a]The cited lysine in this interaction belongs to the X-ray structure of 186–200 segment HSA.
[b]The cited lysine in this interaction belongs to the "750 ps snapshot".
[c]The cited lysine in this interaction belongs to calculation in condensed medium.

section (Section 3.3.3). Table 5 summarizes some lone pair hybridization of species obtained via interactions between bilirubin and the lysines 199 and 195 of HSA. Table 6 illustrates results for atoms hybridization of some of anti-bonding interactions in the aforementioned species. NBO second order energies (ΔE^2_{ij}) for a few donor–acceptor interactions are mentioned in Table 7. ΔE^2_{ij} represents noncovalent delocalization effects which are associated with interactions between filled (donor) and unfilled (acceptor) orbitals. Such interactions are naturally described as being of "donor–acceptor", "charge transfer", or generalized "Lewis base–Lewis acid" type [32].

Numbering system shown for bilirubin, methylamine, protonated methylamine, and acetate in Scheme 4 has been used throughout the NBO analysis.

3.4.1. NBO analysis of the lysine 199 interaction with bilirubin

As is evidenced by the results of Tables 5–7, charge transfer from a sp hybrid orbital and an almost p orbital of O1 of bilirubin to σ-anti-bonding interaction between N3 and H4 belonging to methylamine has occurred. This fact is obvious from ΔE^2_{ij} values of 68.34 and 117.46 kJ/mol in Table 7. These ΔE^2_{ij} values explain charge transfers from oxygen lone pairs Lp(1) O1 with $sp^{1.02}$ hybridization and Lp(2) O1 with $sp^{11.57}$ hybridization as donors to σ-anti-bonding of the N3–H4 (BD*(1) N3–H4) as an acceptor, respectively. This observation is supporting the fact that the interaction of bilirubin with the lysine 199 has caused weakening of the N3–H4 σ-bond in lysine, which can be translated as an undesirable interaction and that a stable species is not obtained from interaction of bilirubin with the lysine 199. One possibility coming to ones mind is whether the charge transfer of $n \rightarrow \sigma^*$ mentioned above could be considered as an H-bonding interaction. As has been reported in literature [37,38], for H-bonding interaction to be seen in N^+–H…O system, two requirements must be met. The oxygen distance from H in N^+–H…O should be about 2.93 Å, while the mentioned three atoms remain collinear. For the species resulting from interaction of the lysine 199 and bilirubin, the observed distance between O1 and H4 is 1.55 Å while, the angle of O1–H4–N3 atoms is about 140°. If one argues that the charge transfer from the lone pairs of oxygen to σ^*_{N-H} can be regarded as a stabilizing interaction, destabilization observed could be assigned to the non-charge transfer interactions. The latter interactions can be regarded as polarizability and induction factors which are caused by electrostatic and exclusion repulsion interactions [32]. It is essential to mention that in the absence of charge transfer interactions, close vicinity of two species is not allowed by electrostatic interaction. So by the aforementioned $n \rightarrow \sigma^*$ charge transfer, the close vicinity of these two species has caused a condition that counteracts a desirable electrostatic interaction.

Table 7
NBO second order interaction energy (ΔE^2_{ij} kJ/mol) for some donor–acceptor interaction of complexes obtained from bilirubin and the amino acid lysines 195 and 199 of the segment 186–200

		ΔE^2_{ij} kJ/mol			
Donor	Acceptor	Lys199-bil[a]	Lys195-bil[a]	Lys195-bil-MD[b]	Lys195-bil-MD[c]
Lp(1) O1	BD*(1) N3–H4	68.34	–	–	73.02
Lp(2) O1	BD*(1) N3–H4	117.46	–	–	–
Lp(1) O2	BD*(1) N2–H2	–	–	29.43	–
Lp(2) O2	BD*(1) N2–H2	–	87.07	96.06	–
Lp(1) O3	BD*(1) N1–H1	–	43.39	–	–
Lp(2) O3	BD*(1) N3–H4	–	116.12	–	–
Lp(2) O4	BD*(1) N4–H5	–	–	–	55.34

[a]The cited lysine in this interaction belongs to X-ray structure of the 186–200 segment HSA.
[b]The cited lysine in this interaction belongs to the "750 ps snapshot".
[c]The cited lysine in this interaction belongs to calculation in condensed medium.

Table 6
Hybridization of some σ-antibonds for interaction of bilirubin with the amino acid lysines 195 and 199 of the 186–200 segment

	Lys199-bil[a]	Lys195-bil[a]	Lys195-bil-MD[b]	Lys195-bil-MD[c]
BD*(1) N1–H1	–	$0.5071sp^{2.23}_N - 0.86195s_H$	–	$0.4782sp^{2.54}_N - 0.8554s_H$
BD*(1) N2–H2	–	$0.4992sp^{1.99}_N - 0.8655s_H$	$0.4588sp^{1.92}_N - 0.8740s_H$	–
BD*(1) N3–H4	$0.4675sp^{2.23}_N - 0.8840s_H$	$0.4884sp^{2.52}_N - 0.8835s_H$	–	–
BD*(1) N4–H5	–	–	–	$0.5263sp^{3.32}_N - 0.8555s_H$

[a]The cited lysine in this interaction belongs to X-ray structure of the 186–200 segment HSA.
[b]The cited lysine in this interaction belongs to the "750 ps snapshot".
[c]The cited lysine in this interaction belongs to calculation in condensed medium.

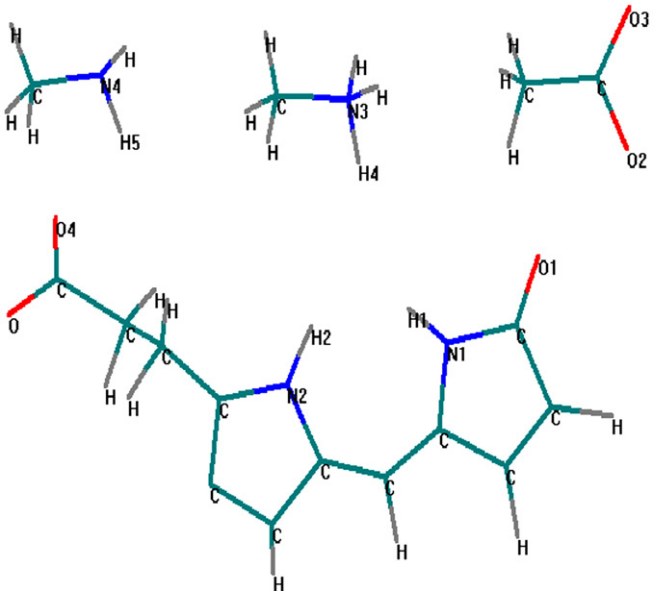

Scheme 4. Numbering system shown for bilirubin, methyl amine and acetate.

3.4.2. NBO analysis of lysine 195 interaction with bilirubin

3.4.2.1. Lysine 195 of the 186–200 segment extracted from X-ray data. As shown in Tables 5–7, it is obvious that charge transfer from an almost p orbital of acetate O2 belonging to the glutamate 188 (Scheme 4) has weakened N2–H2 σ-bond of bilirubin while interacting with the lysine 195 of 186–200 segment extracted from X-ray data. This fact is evident from ΔE^2_{ij} value of 87.07 kJ/mol in Table 7 for interaction of O2 lone pair Lp(2) O2 as donor with σ-anti bonding of N2 and H2 atoms (BD*(1) N2–H2) as acceptor. Similar trends have been observed in weakening of N1–H1 and N3–H4 σ-bonds by charge transfer from a $sp^{0.82}$ hybrid orbital and an almost p orbital of O3 atom of the glutamate 188 (Scheme 4) in above species. These effects are obvious from ΔE^2_{ij} values as 43.39 and 116.12 kJ/mol in Table 7 for interaction of O3 lone pairs (Lp(1) O3, Lp(2) O3) as donors with σ-anti bonding of N1 and H1 atoms (BD*(1) N1–H1), and σ-anti bonding of N3 and H4 atoms (BD*(1) N3–H4) as acceptors, respectively. All above charge transfers are of $n \rightarrow \sigma^*$ character, and since atoms such as N, O and H are involved, hydrogen bonding is plausible. To investigate such H-bonding interactions, we note that the distances of O2 from H1 and H2 in the cited species are 1.79 Å and 1.78 Å respectively. On the other hand, the angles of O2–N1–H1 atoms and of O2–N2–H2 atoms are about 170° and 174° respectively. So charge transfer from O2 lone pairs to N1–H1 and N2–H2 bonds could be considered as a hydrogen bonding interaction between O2, H2 and O2, H1. In the same species the O3, H4 distance is 1.72 Å and the angle of O3–H4–N3 atoms is about 150°. Thus charge transfer from the lone pair of O3 to σ^*_{N3-H4} could be considered as H-bonding interaction too. Based on the above observations, it turns out that the formation of H-bonding by carboxylate group of the glutamate 188 with the lysine 195 and also with bilirubin, has caused protonated ε-NH_2 group of the lysine 195 to distance from the oxygen atom of lactam group of bilirubin. This observation is evident from Scheme 2. As was discussed in previous sections and shown in Table 2, including the acetate group in composite method, the interaction energy rises in the destabilization direction. The interaction energy calculated is of the order of 29 kJ/mol, indicating that the interaction is in the range of H-bonding, in accord to what was explained above. Overall, one comes to the conclusion that bilirubin does not have any interaction with the lysine 195 of the 186–200 segment extracted from X-ray data. Instead, what has been observed suggests that the actual interaction is due to H-bonding involvement of the glutamate 188 with bilirubin.

3.4.2.2. Lysine 195 of the 186–200 segment extracted from the '750 ps snapshot'. As has been shown in Tables 5–7 (last column) and regarding to what was explained above, it is evident that donor–acceptor interaction of bilirubin and lysine 195 of the '750 ps snapshot' has led to the formation of hydrogen bond between O2 and H2. Such effect is apparent from ΔE^2_{ij} values of 29.43 and 96.06 kJ/mol in Table 7 for interaction of a $sp^{0.94}$ hybrid orbital and an almost p orbital of

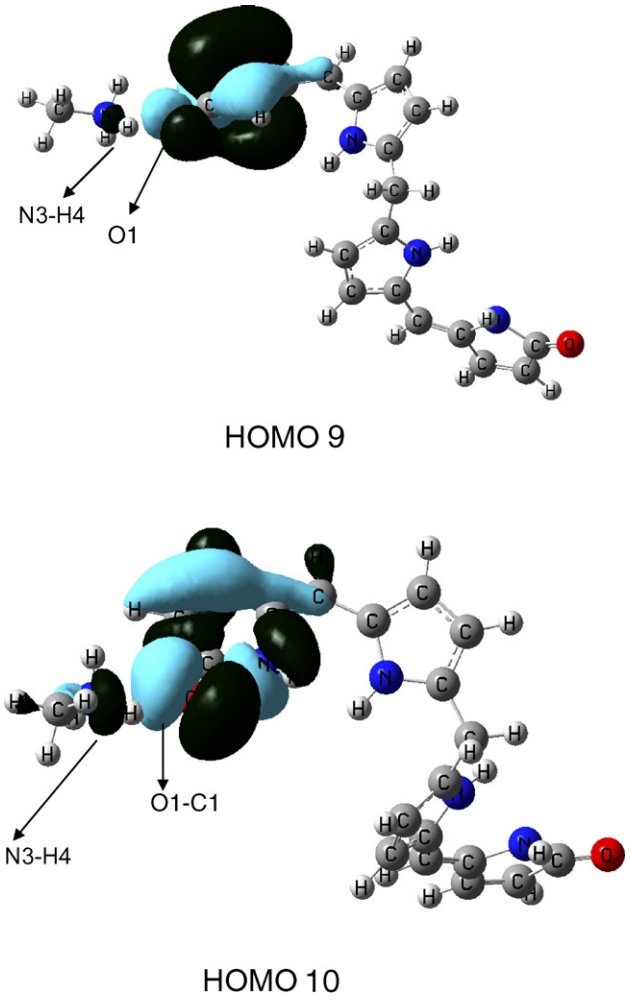

Scheme 5. HOMOs selected for complex obtained from interaction of bilirubin with the lysine 199 belonging to X-ray structure of the 186–200 segment of HSA.

O2 of the glutamate 188 as donors with σ-anti bonding of N2 and H2 atoms (BD*(1) N2–H2) of bilirubin as acceptor, respectively. In accord to n → σ* charge transfer just mentioned, O2–H2 distance of 1.75 Å and O2–H2–N2 angle of 168° lend support to H-bonding interaction suggested above. Contrary to the previous section, no H-bonding is seen to form between O3 of glutamate and ε-NH_3 group of the lysine 195 in the present case. This phenomenon is due to the simulation process, which has caused the glutamate 188 to distance from the lysine 195. Thus a favorable electrostatic interaction of bilirubin with the lysine 195 has been achieved when H-bonding between the glutamate 188 and the lysine 195 is lost. This latter effect is evident from the improvement in interaction energy of Table 4, which can be attributed to a more accurate evaluation of electrostatic interaction of the lysine 195 with bilirubin, as well as H-bonding between the glutamate 188 and bilirubin. Moreover, since based on NBO results, no bonding interaction between the lysine 195 and bilirubin has been observed an interaction energy of about 200 kJ/mol is indicative of an electrostatic interaction of the two species.

3.4.2.3. Lysine 195 of IIA subdomain in condensed medium calculations. According to what was explained based on Scheme 3, present NBO analysis has been restricted just to interaction of lysine 195 and bilirubin as the only remaining interaction site. The latter sites in lysine 195 are limited to ε-NH_3^+ and its α-NH groups. Thus to simplify matters and in accord to other sections, methyl amine and protonated methyl amine are substituted with lysine 195 which interact with oxygen atom of lactam group and oxygen of –COO of bilirubin, respectively. Tables 5–7 summarize the NBO results using the numbering system shown in Scheme 3 which include donor–acceptor interaction for N3–H4 and N4–H5 bonds with lone pairs of O1 and O4 respectively. This fact is apparent from ΔE_{ij}^2 values of 73.02 and 55.34 kJ/mol in Table 7 for interaction of a $sp^{0.74}$ hybrid orbital of O1 and a p orbital of O4 of bilirubin as donors

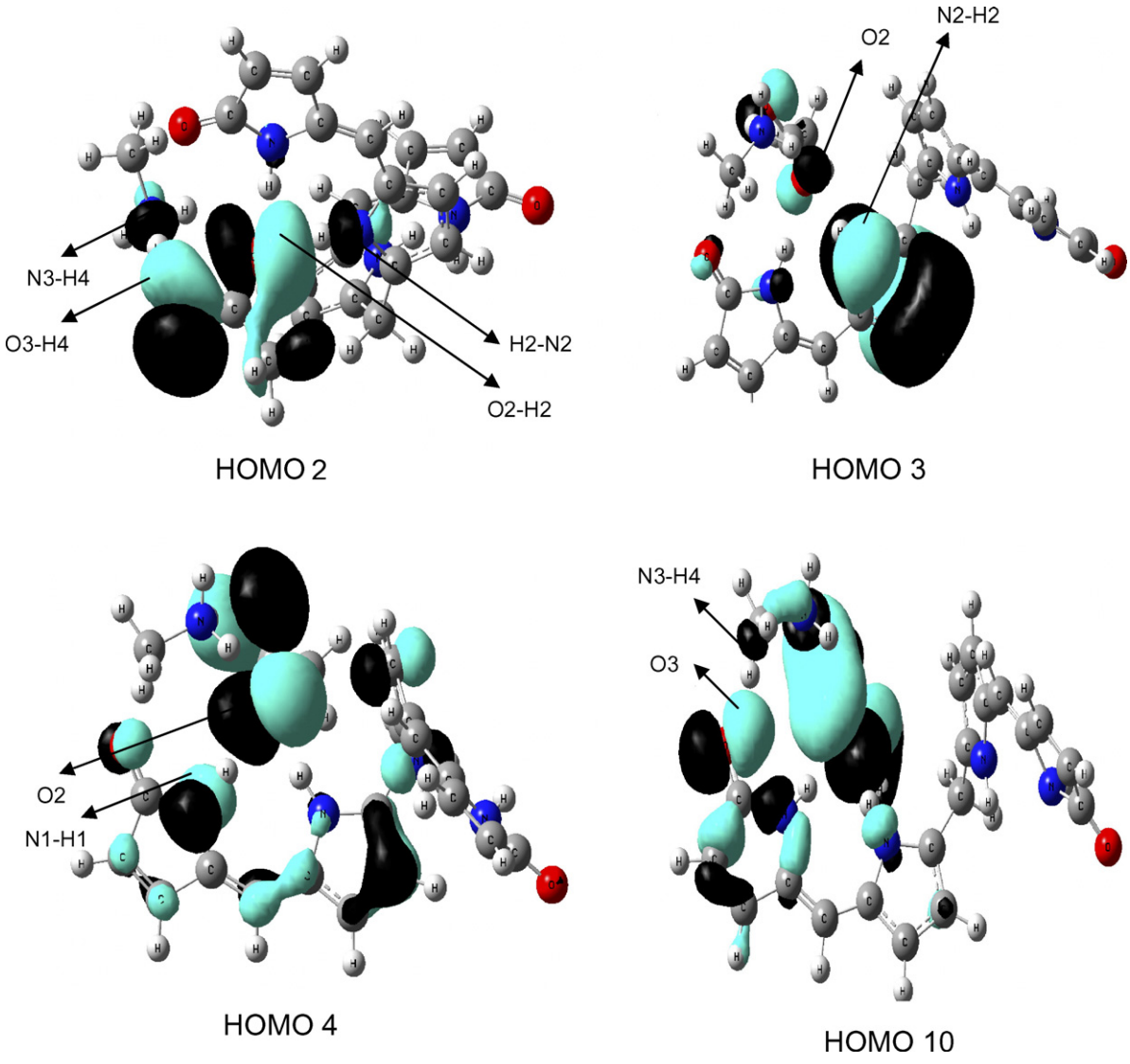

Scheme 6. HOMOs selected for complex obtained from interaction of bilirubin with the lysine 195 belonging to X-ray structure of the 186–200 segment of HSA.

with σ-anti bonding of N3 and H4 atoms (BD*(1) N3–H4) and N4 and H5 atoms (BD*(1) N4–H5) of lysine 195 as acceptor, respectively. Regarding the distance observed between H4 and O1 (1.75 Å), and O1–H4–N3 angle (158.2°), and based on the interactions just described, a hydrogen bonding between ε-NH_3^+ group of lysine and lactam oxygen of bilirubin has been formed. Besides, distance of 1.9 Å between O4 and H5 and 140.4° angle of O4–H5–N4 suggest a weaker hydrogen bonding interaction between α-NH group of lysine with –COO group of bilirubin. The above data confirm that in the interaction of bilirubin with HSA, besides the electrostatic interaction between lysine 195 and bilirubin, which is due to ε-NH_3^+ group of lysine 195 being adjacent to lactam oxygen of bilirubin, hydrogen bonding plays a definite role in the interaction.

3.5. Molecular Orbital (MO) analysis

Molecular orbital calculations have been carried out for all species included in Tables 5–7. The MO's obtained as shown in Schemes 5–8 are studied in support of NBO analysis. HOMO-9 and 10 of lysine 199–bilirubin complex have been shown in Scheme 5. HOMO-9 of this species shows antibonding interactions between a lobe of p orbital of O1 atom and electronic cloud over N3 and H4 atoms. In HOMO-10 of this species, the phase combination of C1, O1 orbitals have an antibonding interaction to electronic cloud over N3 and H4 atoms. These HOMOs indicate that due to neighboring of ε-NH_3^+ group of lysine and O1 atom of lactam ring of bilirubin, weakening of N3–H4 σ-bond occurs conforming NBO analysis. HOMOs 2, 3, 4, and 10 of bilirubin–lysine 195 species (lysine 195 obtained from 186–200 segment extracted from IIA X-ray structure) have been illustrated in Scheme 6. HOMO-2 of this species shows the localized electronic density between O3 and H4 in opposite phase to the electronic cloud along the N3–H4 bond. The same HOMO reveals that a phase combination of orbitals between O2 and H2 has occurred such that it shows an opposite phase with the electronic cloud along the N2–H2 bond of bilirubin's pyrrol ring. Also phase combination of orbitals between O2 and H2 have an

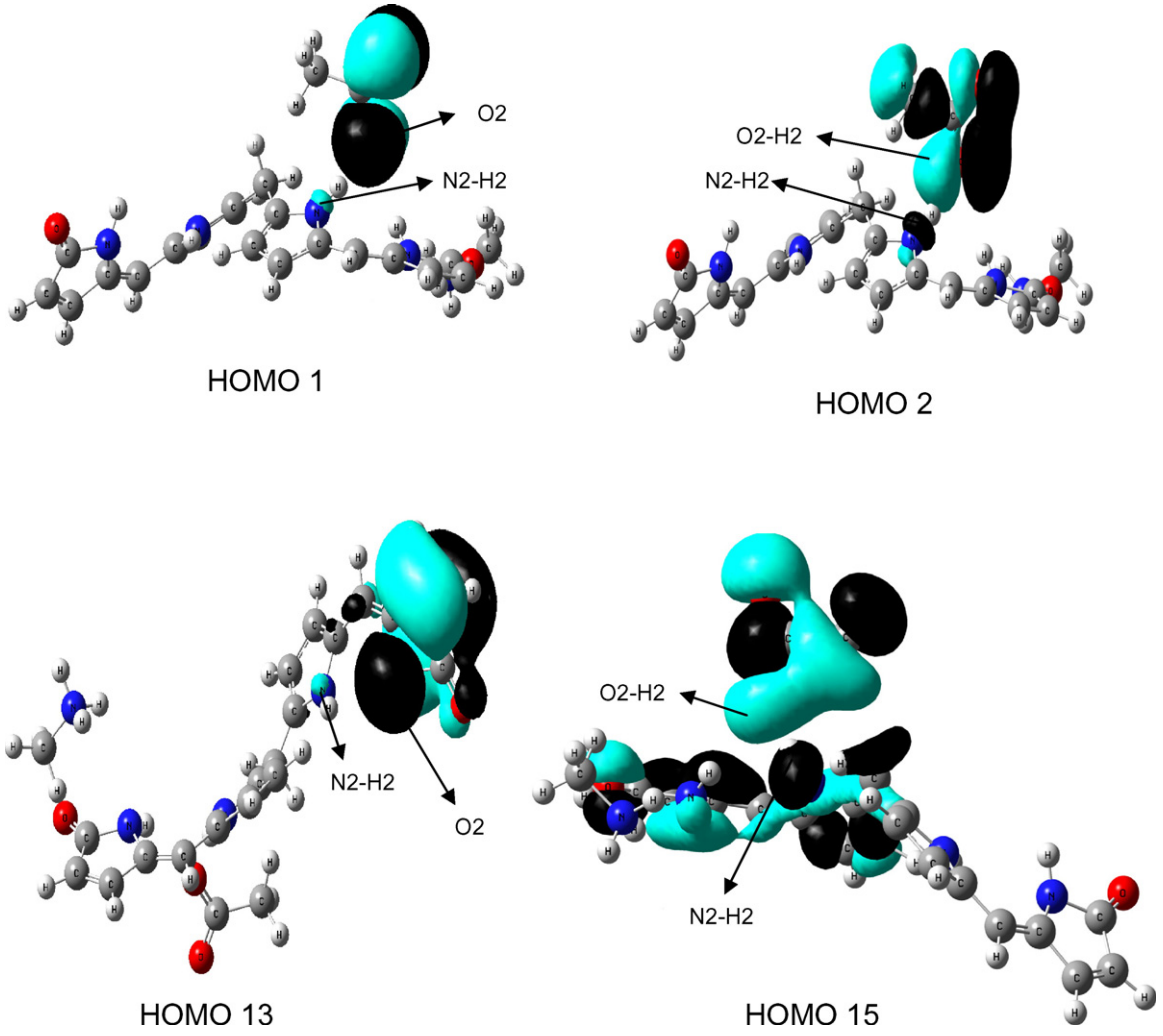

Scheme 7. HOMOs selected for complex obtained from interaction of bilirubin with the lysine 195 from the "750 ps snapshot" of molecular dynamic simulated HSA structure.

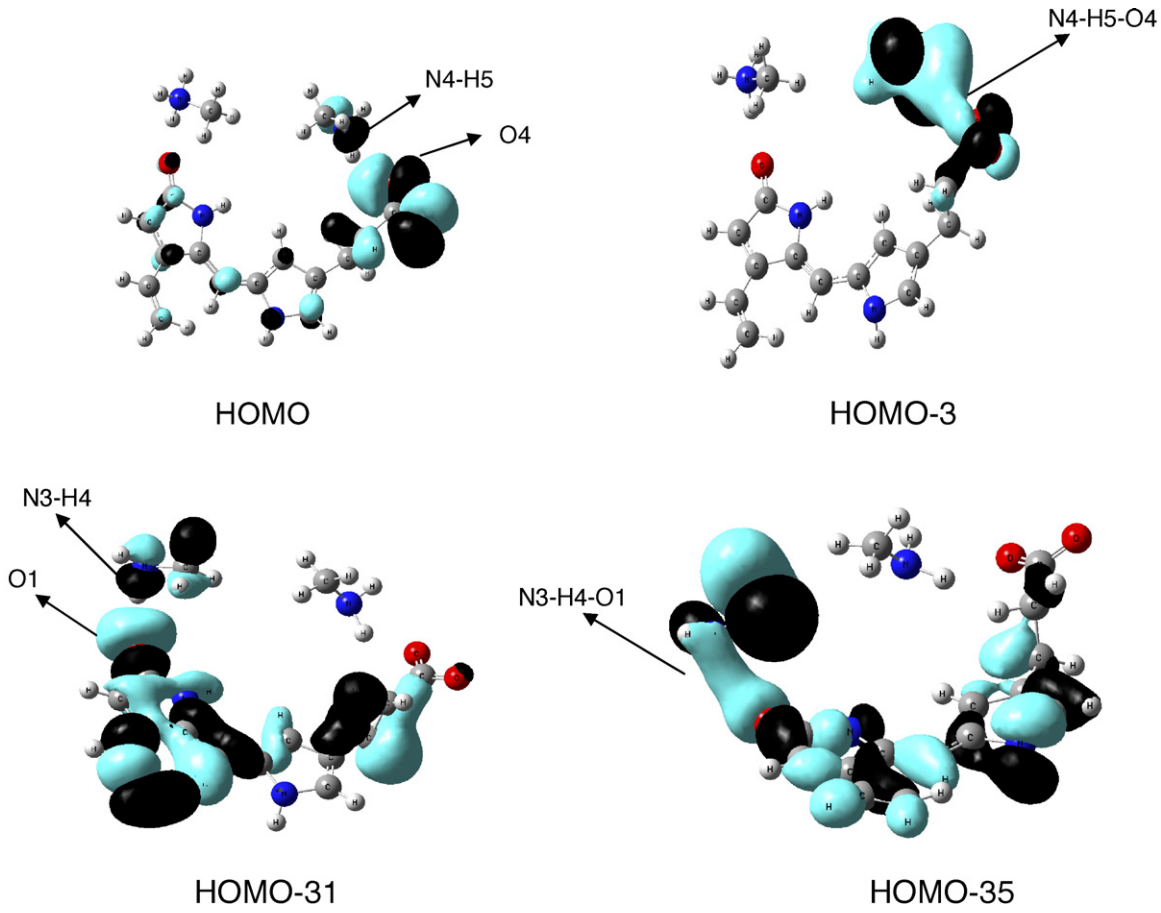

Scheme 8. HOMOs selected for complex obtained from interaction of bilirubin with the lysine 195 from condensed medium calculations.

antibonding interaction with p orbital of O2 as shown in HOMO-3 of the same complex (Scheme 6). Whereas, in HOMO-4 the aforementioned interaction is observed for O2 atom and N1–H1 bond of bilirubin. HOMO-10 of this species indicates an antibonding interaction between a lobe of O3 p orbital with an electronic cloud of bond between N3 and H4 atoms. As a result of such observations, we can conclude that HOMOs 2, 3, and 4 together show H-bonding interaction of glutamate 188 with bilirubin. This effect can be supported by bond angles observed for O2–N2–H2 and O2–N1–H1 atoms being equal to about 174° and 170° respectively. HOMO-2 and -10 together indicate an H-bonding formation between lysine 195 and glutamate 188 taking into account the O3–H4–N3 angle of 150°.

A few HOMOs of bilirubin interaction with lysine 195 of 186–200 segment extracted from '750 ps snapshot' have been illustrated in Scheme 7. From HOMO-1, an antibonding interaction of p orbital of O2 with the phase combination of orbitals along N2–H2 atoms is apparent. The same interaction can be observed in HOMO-2 and -15 for an electronic cloud over O2–H2 with a cloud over N2 and H2 bond. HOMO-13 is indicative of an antibonding interaction of π electronic cloud on O2 atom with a phase combination of orbital on N2 and H2 atoms. With regard to the angle between O2–N2–H2 atoms in above species being equal to 168°, the above HOMOs all illustrate an H-bonding interaction between bilirubin and the glutamate 188. These facts are all in accord to the NBO analysis results.

HOMOs illustrated in Scheme 8 refer to the interaction of lysine 195 with bilirubin which have been obtained from the calculations of such interaction in condensed medium. HOMO shows an antibonding interaction of p orbital of O4 with the phase combination of orbitals along the N4–H5 bond. On the other hand, in HOMO-3 (also in HOMO-25 and HOMO-26 which are not shown) a phase combination of orbitals over N4–H5–O4 is evident. Taking the position of three atoms O4, H5, and N4 into account, the latter two MOs can be regarded as a supporting evidence of the presence of a hydrogen bonding with the participation of the mentioned atoms. HOMO-31 indicates an antibonding interaction of a hybrid orbital of O1 with the phase combination of orbitals along the N3–H4 bond. Besides, in HOMO-35 (also in HOMO-36 and HOMO-41 which are not shown) a phase combination of orbitals over N3–H4–O1 is obvious. Regarding the position of three atoms O1, H4, and N3 into account, the latter two MOs can be considered as a supporting evidence of the presence of an even stronger hydrogen bonding with the participation of the mentioned atoms. In both hydrogen bonding cases, the N–H bond distance has been lengthened by 5–10%. Therefore, MO analysis fully supports the results of NBO calculations.

4. Conclusion

This work has been an attempt to determine the primary site of HSA upon interaction with bilirubin using molecular dynamic simulations, QM and QM/MM minimization methods. In order to accomplish such task, two computational schemes have been employed. In the first approach based on previous experimental works, a pre-optimized segment 186–200 of HSA has been chosen and its interaction with bilirubin investigated. The aforementioned segment has once been obtained from X-ray structure of subdomain IIA, while another time has been achieved from simulation on subdomain IIA of HSA in vacuum. In order to reduce the computational cost, the presence of ions and water molecules has been neglected in this approach, while such species have been accounted for in the other approach. Interaction of bilirubin with lysine residues 190, 195, and 199 of the 186–200 segment reported as first candidates in literature, selected from subdomain IIA, have been investigated both before and after the simulation in vacuum using quantum mechanical calculations. In order to reduce the computational cost, and knowing the fact that the ethyl side groups do not intervene in the interaction of bilirubin with lysine residues, they have been replaced by hydrogen atoms. Since the lysine 190 is neutral, it has been protonated in order to investigate its electrostatic interaction with bilirubin. Results obtained for bilirubin interaction with the lysine residues in the 186–200 segment extracted from X-ray structure have shown that the lysine 190 and 195 residues can remain as potential candidates for such interaction. A molecular dynamic simulation in vacuum on IIA subdomain of HSA, with the aim of reaching to a better agreement with the experimental observations, has been performed. The final optimized geometry reached for the 186–200 segment after simulation has revealed that the lysine 190 is not capable of holding a proton. It is noticed that due to folding of the simulated segment, achieving an optimized geometry for the lysine 199 and bilirubin interaction has been fruitless. As a result, in accord to the previous experimental reports, the lysine 195 holds the sole electrostatic site of interaction with bilirubin. NBO analysis results suggest that tasks to achieve a structure indicating bilirubin interaction with the lysine 195 from 186–200 segment extracted from X-ray structure, results in a structure that lacks any electrostatic interaction. In fact, it has been found that stability of the latter species can be attributed to the H-bonding interaction of the glutamate 188 with both bilirubin and the lysine 195. Further NBO analysis on the structure of the same species while achieved after molecular dynamic simulation on subdomain IIA has revealed that a favorable electrostatic interaction between the lysine 195 and bilirubin has occurred. Besides, H-bonding interaction of the glutamate 188 with bilirubin has been evident in the same species. For the second approach, HSA was initially placed in a water and ion box. By bilirubin docking primary structures for bilirubin HSA interaction were obtained. Results achieved from docking treatment led us to IIA subdomain dissection of HSA. Advancing with a simulated annealing treatment followed by a QM/MM minimization, a structure for interaction of lysine 195 with bilirubin was obtained. Results suggest that although bilirubin could essentially show interaction with all lysine residues as well as glutamates 13, the only apparent remaining bilirubin interaction is with lysine 195. Above data confirm that in the interaction of bilirubin with HSA, besides the electrostatic interaction between lysine 195 and bilirubin, which is due to ε-NH_3^+ group of lysine 195 being adjacent to lactam oxygen of bilirubin, hydrogen bonding plays a definite role in the interaction. Molecular orbital calculations have been presented which support the NBO analysis. As has been pointed out, based on the simulation in vacuum results, it is expected that accounting the condensed medium would not affect the relative interaction behavior of lysine residues with bilirubin, namely it is just sufficient to consider the lysine 195 interaction. But more accurate evaluation of above interaction can be achieved just with calculations in the condensed medium because more flexibility may be experienced in the relative position of lysine 195 and bilirubin. The ultimate conclusion is that the gas phase calculation can provide a qualitative assessment of the relative interaction of various sites of protein with a ligand when those sites indicate a large different behavior. Although even in this case the atoms configurations in the interaction core are not in accord to that of a real model obtained from condensed medium calculation.

Acknowledgment

We are grateful to Professor Seik Weng Ng for making available to us his software (G98W) and hardware (machine time) facilities. The financial support of the Research Councils of Shahid Beheshti University and the University of Tehran are gratefully acknowledged.

References

[1] R.F. Chen, Arch. Biochem. Biophys. 160 (1974) 106–112.
[2] R.L. Levine, Clin. Chem. 23 (1977) 2292–2301.
[3] R. Schmid, I. Diamond, L. Hammaker, C.B. Gundersen, Nature 206 (1965) 1041–1043.
[4] T. Faerch, J. Jacobsen, Arch. Biochem. Biophys. 184 (1977) 282–289.
[5] R.D. Gray, D.S. Stroupe, J. Biol. Chem. 253 (1978) 4370–4377.
[6] H. Athar, N. Ahmad, S. Tayyab, M.A. Ghasim, Int. J. Biol. Macromol. 25 (1999) 353–358.
[7] J. Jacobsen, FEBS Lett. 5 (1969) 112–114.
[8] G.H. Beaven, A. d'Albis, W.B. Gratzer, Eur. J. Biochem. 33 (1973) 500–510.
[9] C. Jacobsen, Eur. J. Biochem. 27 (1972) 513–519.
[10] H. Murakawa, J. Mabe, A. Seki, J. Mol. Struct. 297 (1993) 41–48.
[11] J. Jacobsen, Int. J. Pept. Protein Res. 9 (1977) 235–239.
[12] S. Tayyab, M.A. Qasim, Biochem. Int. 18 (1989) 343–349.
[13] M.M. Mir, K.M. Fazili, M. Abul Qasim, Biochim. Biophys. Acta 1119 (1992) 261–267.
[14] J. Jacobsen, R. Brodersen, J. Biol. Chem. 258 (1983) 6319–6326.
[15] D.C. Carter, X.M. He, Nature 358 (1992) 208–215.
[16] D.C. Carter, J.X. Ho, Adv. Protein Chem. 45 (1994) 153–201.
[17] R.G. Reed, R.C. Feldhoff, O.L. Clute, T. Peters Jr., Biochemistry 14 (1975) 4578–4583.
[18] C. Jacobsen, Biochem. J. 171 (1978) 453–459.
[19] C.E. Petersen, C.E. Ha, K. Harohalli, J.B. Feix, N.V. Bhagavan, J. Biol. Chem. 275 (28) (2000) 20985–20995.
[20] C.B. Berde, B.S. Hundson, R.D. Simoni, R.D. Sklar, J. Biol. Chem. 254 (1979) 391–400.

[21] D.A. Lightner, W.M.D. Wijekoon, M.H. Zhang, J. Biol. Chem. 263 (1988) 16669–16676.
[22] N. Roosdorp, B. Wann, I. Sjoholm, J. Biol. Chem. 252 (1977) 3876–3880.
[23] S. Sugio, A. Kashima, S. Mochizuki, M. Noda, K. Kobayashi, Protein Eng. 12 (1999) 439–446.
[24] M.J. Frisch, et al., Gaussian 98 (Revision A.9), Gaussian Inc., Pittsburgh PA, 1998.
[25] A.D. Becke, J. Chem. Phys. 98 (1999) 5648–5652.
[26] G.A. Peterson, M.A. Al-laham, J. Chem. Phys. 94 (1991) 6081–6091.
[27] J.J.P Stewart, J. Comp. Chem. 10 (1989) 221–264.
[28] D. van der Spoel, E. Lindahl, B. Hess, A.R. van Buuren, E. Apol, P.J. Meulenhoff, D.P. Tieleman, A. Sijbers, K.A. Feenstra, R. van Drunen, H.J.C. Berendsen, Department of Biophysical Chemistry, University of Groningen, The Netherlands, 2001–2004.
[29] W.F. van Gunsteren, S.R. Billeter, A.A. Eising, P.A. Hünenberger, P. Krüger, A.E. Mark, W.R.P. Scott, I.G. Tironi, Biomolecular Simulation, the GROMOS96 Manual and User Guide, Hochschulverlag AG der ETH, Zürich, 1996.
[30] G. Groenhof, M.F. Lensink, H.J.C. Berendsen, J.G. Snijders, A.E. Mark, Proteins 48 (2002) 202–211.
[31] G. Groenhof, M.F. Lensink, H.J.C. Berendsen, A.E. Mark, Proteins 48 (2002) 212–223.
[32] A.E. Reed, L.A. Curtiss, F. Wienhold, Chem. Rev. 88 (1998) 899–926.
[33] N. Diaz, D. Suarez, T.L. Sordo, K.M. Merz, J. Am. Chem. Soc. 123 (2001) 7574–7583.
[34] K. Raghavachari, L.A. Curtiss, in: D.R. Yarkony (Ed.), Modern Electronic Structure Theory Part II, World Scientific, Singapore, 1995.
[35] Z. Moosavi-Movahedi, S. Safarian, M. Zahedi, M. Sadeghi, A.A. Saboury, J. Chamani, H. Bahrami, A. Ashraf-Modarres, A.A. Moosavi-Movahedi, The Protein Journal (in press) doi:10.1007/s10930-006-9002-y.
[36] N. Diaz, D. Suarez, T.L. Sordo, K.M. Merz, J. Med. Chem. 44 (2) (2001) 250–260.
[37] L. Stryer, J.M. Berg, J.L. Tymokzko, Biochemistry, W.H. Freeman and Company, New York, 1988.
[38] R. Chang, Physical Chemistry with Application to Biological Systems, Collier Macmillan, New York, 1981.